

Spiral Motion in a Noisy Complex Ginzburg-Landau Equation

Igor S. Aranson^(a), Hugues Chaté^(b), and Lei-Han Tang^(c)

^(a) *Materials Science Division, Argonne National Laboratory, Argonne, IL 60439, USA*

^(b) *CEA — Service de Physique de l'Etat Condensé, Centre d'Etudes de Saclay, 91191 Gif-sur-Yvette, France*

^(c) *Department of Physics and Center for Nonlinear and Complex Systems, Hong Kong Baptist University, Hong Kong*

(November 15, 2018)

The response of spiral waves to external perturbations in a stable regime of the two-dimensional complex Ginzburg-Landau equation (CGLE) is investigated. It is shown that the spiral core has a finite mobility and performs Brownian motion when driven by white noise. Combined with simulation results, this suggests that defect-free and quasi-frozen states in the noiseless CGLE are unstable against free vortex excitation at any non-zero noise strength.

PACS: 68.55.-a, 05.70.Ln, 81.10.Aj, 85.40.Ux

Vortices play a central role in the ordering of two-dimensional equilibrium systems characterized by a complex scalar order parameter, e.g., planar magnets and Bose-condensates [1]. They also arise in various nonequilibrium situations, e.g., the Belousov-Zhabotinsky reaction, certain regimes of fluid flows, and the contraction of heart muscles [2–5]. Their long-time motion is determined by their coupling to the slow modes of the system, and hence is expected to acquire a universal character.

A distinctive but common feature exhibited by a vortex in a nonequilibrium oscillating state is the emission of spiral waves which change the oscillating frequency of the entire system. This behavior is seen, e.g., from solutions of the generic model for these situations, the complex Ginzburg-Landau equation (CGLE) [2,4]:

$$\partial_t a = a - (1 + ic)|a|^2 a + (1 + ib)\nabla^2 a, \quad (1)$$

where $a(\mathbf{x}, t)$ is a complex scalar field, and b and c are real numbers. Spiral waves are observed for any $b \neq c$. In certain regimes of the parameter space (b, c) , spiral defects are spontaneously generated and undergo violent motion, while in other cases they are quite static and lock into a quasi-frozen structure [6].

In this Letter, we derive mobility relations for a single spiral in the regime of Eq. (1), where the uniformly oscillating state as well as spiral wave excitations are linearly stable. We show that, in contrast to the equilibrium XY model (which corresponds to $b = c = 0$), a vortex defect possesses a nonzero mobility and responds only to perturbations which fall within a distance ξ , the “screening length”, from the spiral core. When a noise source is present, the above property yields a diffusion constant D for the spiral core proportional to the noise strength. The diffusion constant D is calculated through a numerical scheme with the result well in accord with direct simulations of a noisy CGLE. Secondly, we present simulation results to show that both the defect-free state and the frozen-defect state of the noiseless CGLE disappear when the (thermal) noise is introduced. These findings are rationalized in the context of noise-driven vortex diffusion

and thermally-activated nucleation of vortex-antivortex pairs. We believe the analysis will help toward understanding various other regimes exhibited by the noiseless CGLE, in particular, the melting of the frozen-defect state into the defect-turbulence state.

A single-spiral solution to Eq. (1) is well documented [7,8]. For a single-charged vortex centered at \mathbf{x}_0 , the solution takes the form,

$$a_s(\mathbf{x}, t) = F(r) \exp[i(\theta + \psi(r) - \omega t)], \quad (2)$$

where $r = |\mathbf{x} - \mathbf{x}_0|$ and θ is the polar angle measured from the vortex core. Far away from the core, the solution approaches a plane wave with $\psi(r) \simeq kr$, where the asymptotic wavenumber k is related to the rotation frequency as $\omega = c + (b - c)k^2$. The dependence of k on b and c is known analytically for $|b - c| \ll 1$ and $|b - c| \gg 1$, e.g. $k \simeq -c^{-1} \exp(-\pi/|2c|)$ for $b = 0$ and $|c| \ll 1$ [7].

In the following discussion, we shall limit ourselves to the case $b = 0$ and $c \neq 0$. This choice is partly motivated by a desire for simplicity, but it also offers an interesting framework: all plane waves of wavenumber $k < k_c(c) = (3 + 2c^2)^{-1/2}$ are linearly stable in this case, including the homogeneous state $a = \exp(-ict)$ at $k = 0$. For $c < c_i \simeq 1.08$, an isolated spiral is stable and has a wavevector $k < k_c$ [9]. In the case $b = c = 0$, Eq. (1), in the presence of noise, reduces to the Ginzburg-Landau equation for a superfluid (or a planar magnet), allowing the crossover between the equilibrium XY model and the nonequilibrium CGLE to be explored. In addition, increasing c , solutions of (1) show a transition from the quasi-frozen state to the “defect turbulence” state [6], which can then be probed in the presence of noise.

We now consider the response of the spiral to a weak additive broad-band noise $\eta(\mathbf{x}, t)$,

$$\partial_t a = a - (1 + ic)|a|^2 a + \nabla^2 a + \eta(\mathbf{x}, t). \quad (3)$$

To the linear order in η , we can write the perturbed solution in the form,

$$a(\mathbf{x}, t) = a_s(\mathbf{x}, t) + \int d\mathbf{x}' dt' g_s(\mathbf{x}, t; \mathbf{x}', t') \eta(\mathbf{x}', t'), \quad (4)$$

where $g_s(\mathbf{x}, t; \mathbf{x}', t')$ is the Green's function for the CGLE linearized around $a_s(\mathbf{x}, t)$. Although the exact form of g_s can only be obtained numerically, it is instructive to examine its behavior when \mathbf{x}' is far away from the spiral core. This can be done as follows.

In the far field, the spiral wave is very close to a planewave with a wavevector $\mathbf{k} = k\hat{\mathbf{e}}_r$. Correspondingly, the inhomogeneous Green's function g_s at large distances can be approximated by the Green's function g_p of the planewave. The planewave Green's function can be decomposed into contributions from two types of modes, the amplitude modes with a time constant of order one, and the soft phase modes. Only the latter part survives at long times, yielding the asymptotic expression,

$$g_p(\mathbf{x} + \mathbf{x}_0, t + t_0; \mathbf{x}_0, t_0) \sim \frac{\exp[i(\mathbf{k} \cdot \mathbf{x} - \omega t)]}{4\pi t \alpha_{\parallel}^{1/2}} \times \exp\left[-\frac{x_{\perp}^2}{4t} - \frac{(x_{\parallel} - v_g t)^2}{4\alpha_{\parallel} t}\right], \quad (5)$$

where x_{\parallel} and x_{\perp} are parallel and perpendicular components of \mathbf{x} with respect to \mathbf{k} , and $\alpha_{\parallel} = 1 - 2(1 + c^2)k^2/(1 - k^2)$. (Convective instability sets in at $\alpha_{\parallel} = 0$.) The group velocity of the plane-wave is given by $\mathbf{v}_g = \nabla_{\mathbf{k}}\omega = -2c\mathbf{k}$.

Equation (5) implies that a localized perturbation spreads diffusively but, at the same time, its center travels at the group velocity \mathbf{v}_g . Equating $v_g t$ with the diffusion length $t^{1/2}$, we obtain a length $\xi \simeq v_g^{-1} \simeq |ck|^{-1}$. This is the decay length of disturbances in the “upstream” direction (i.e., against \mathbf{v}_g), beyond which the influence becomes exponentially small at any time. Thus only perturbations within the distance ξ from the spiral core can have a significant influence on its motion. This is in contrast with the equilibrium XY model ($c = 0$ and $v_g = 0$), where the effect of disturbances far away decays only algebraically with the distance.

A quantitative analysis of the spiral motion under the perturbation η can be done by decomposing the correction term in (4) into two parts: (i) shape change of the spiral wave, and (ii) translation $\mathbf{x}_0 \rightarrow \mathbf{x}'_0$ and shift of the overall phase $\psi_0 \equiv \psi(0) \rightarrow \psi'_0$. Since the unperturbed spiral wave is stable, the first type of response decays in time when the perturbation is switched off. On the other hand, the second type of response corresponds to the zero modes of the unperturbed spiral solution and hence does not decay away. Under an infinitesimal translation of the core position $\mathbf{x}_0 = (x_0, y_0)$, the spiral solution changes to $a'_s = a_s + x_0 w_x + y_0 w_y$, where w_x and w_y are the translational zero modes in the x and y direction, respectively. They are solutions of Eq. (1) linearized around a steady spiral, Eq. (2). In the presence of the noise η , the equations for the translation zero modes assume the form:

$$\dot{x}_0 = \zeta_x, \quad \dot{y}_0 = \zeta_y, \quad (6)$$

where ζ_x and ζ_y are projections of η on the zero modes w_x and w_y , respectively.

While the form of the functions w_x and w_y can be obtained directly by differentiating (2), the calculation of ζ_x and ζ_y is quite difficult. This is because the operator \mathcal{L} which defines the linearized equation around a spiral solution is non-hermitian except at $c = 0$, so the eigenfunctions u_{α} , $\alpha = x, y$, of the adjoint operator \mathcal{L}^{\dagger} are in general different from the eigenfunctions w_{α} . For $c \sim 1$, we have developed a numerical scheme [10] to determine u_{α} , details of which will be reported elsewhere [11]. Quite generally, $u_{\alpha}(r, \theta)$ decays exponentially at large distances from the spiral core [8]. From the projection formula,

$$\zeta_{\alpha} = \frac{\int d^2x u_{\alpha}^{\dagger} \eta}{\int d^2x u_{\alpha}^{\dagger} w_{\alpha}}, \quad (7)$$

we see that only the part of the perturbation η sufficiently close to the core contributes to ζ_{α} , in accord with the qualitative analysis developed above. The exponential decay of u_{α} also ensures the convergence of the integral on the denominator, yielding a finite “mobility” to the spiral core. This contrasts with the $c = 0$ case, where the integral diverges, and the vortex mobility decreases logarithmically with the relevant length scale.

We now apply the above discussion to the special case where the external perturbation takes the form of a weak, uncorrelated white noise with zero mean and correlators,

$$\langle \eta_{\beta}(\mathbf{x}, t) \eta_{\gamma}(\mathbf{x}', t') \rangle = 2T \delta_{\beta\gamma} \delta(t - t') \delta(\mathbf{x} - \mathbf{x}'), \quad (8)$$

where β, γ specify real and imaginary parts of η and T characterises the noise strength. Solving Eq. (6), we obtain a diffusion law for the vortex core at long times,

$$\langle [\mathbf{x}_0(t) - \mathbf{x}_0(0)]^2 \rangle = 4Dt. \quad (9)$$

For small T , the diffusion constant is $D = \mu T$, with the mobility given by

$$\mu = \frac{\int d^2x u_x^{\dagger} u_x}{|\int d^2x u_x^{\dagger} w_x|^2}. \quad (10)$$

We have evaluated Eq. (10) for several different values of c using the numerically determined eigenfunctions u_{α} and w_{α} , and have also performed Langevin simulations of the noisy CGLE (3). In the simulations, the core coordinates of an initially prepared spiral was followed in time at various noise strengths T . Brownian motion of the core was observed. In Fig. 1(a), we show the simulation data for the mean-square deviation of the core coordinates versus time for $c = 1.4$ and various values of temperature T . From the slope of the curves, we determine the diffusion constant D , which is found to vary linearly with T at small T . In Fig. 1(b), we plot the mobility μ against the parameter c , where filled squares correspond to data obtained from simulations, and open circles data from direct calculations using Eq. (10). The agreement between the two sets is apparent.

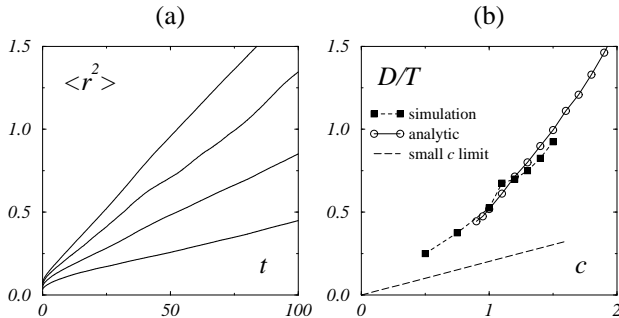


FIG. 1. Noise-driven spiral diffusion: (a) mean-square displacement $\langle r^2 \rangle = \langle [\mathbf{x}_0(t) - \mathbf{x}_0(0)]^2 \rangle$ vs. time for $c = 1.4$, $T = 0.001, 0.002, 0.003$, and 0.004 (from bottom to top). Data obtained from the trajectory, over $\Delta t \sim 10^4$, of a spiral initially centered in a disk of radius 128 with no-flux boundary conditions. (b) mobility $\mu = D/T$ vs. c .

In the special case $c = 0$, the problem reduces to that of vortex diffusion in an equilibrium XY model, which has been studied extensively in the past. In this case, the linear operator \mathcal{L} becomes hermitian, and $u_\alpha = w_\alpha$. For $|c| \ll 1$, we have analyzed the eigenvalue equation for u_α in detail, and found that $u_\alpha \simeq w_\alpha$ at distances up to $r \sim \xi$ before it switches over to exponential decay at $r > \xi$. Using this property and the exponential divergence of ξ for $c \rightarrow 0$, we obtain

$$\mu \simeq 2c/\pi^2. \quad (11)$$

We have checked that this small c behavior is consistent with the trend exhibited by the numerical data shown in Fig. 1, though the next order term is significant when c reaches a value of order one.

The discussion presented above on the diffusivity of a single vortex serves as a useful basis for understanding the behavior of the noisy CGLE (3) under more general initial conditions. Specifically, we have examined numerically the behavior of the system under two representative initial conditions: (a) a uniform, defect-free state with $a = 1$, and (b) a random initial state with $|a| \ll 1$. (In the latter case the system initially develops into a configuration with a high density of vortices.) It has been shown that, in the absence of noise, case (a) is stable and the system remains synchronized (i.e., with bound or no phase fluctuations) at all times, while case (b) evolves into a “quasifrozen-defect” state for $c < c^* \simeq 1.68$ and a “defect-turbulence” state for $c > c^*$ [6]. Our simulations show that, when noise is present, the distinction disappears and the system evolves into a single steady-state with a finite density of vortices.

Figure 2 shows the breakdown, under weak noise ($T = 0.002$), of an initially-blocked configuration [Fig. 2(a)] obtained at $c = 1.4$ by simulating the noiseless equation with a random initial condition. Clear spots with a black center indicate the depression of $|a|$ at the vortex cores. Switching on the noise, we see the diffusive motion of individual vortices, creation of new vortices—in this case, through noise amplification by a convective instability

[clear belt in the lower left corner in Fig. 2(b)]—, and annihilation of vortex-antivortex pairs. For weaker noise, the whole process occurs on larger timescales, reaching an asymptotic state with larger spirals.

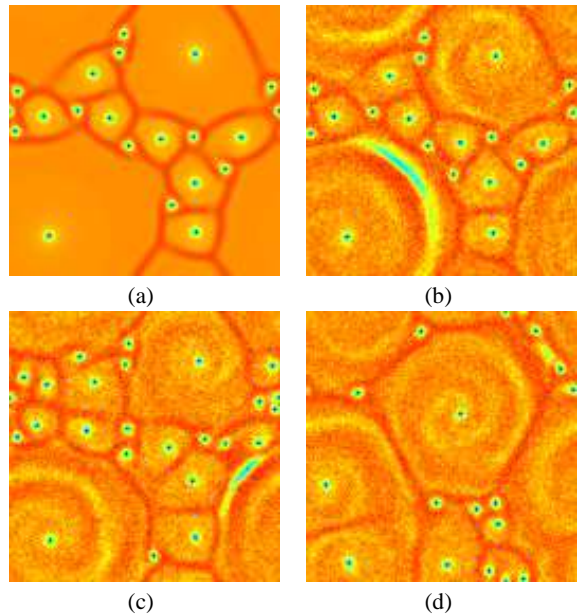


FIG. 2. Snapshots of $|a|$ during the breakdown of a blocked configuration at $c = 1.4$. System of linear size $L = 128$ with periodic boundary conditions. (a): blocked state ($T = 0$). (b,c): initial stages ($T = 0.002$, $t \sim 500, 700$); note the $|A|$ modulations emitted by the cores of the large spirals. (d): in the asymptotic state ($T = 0.002$, $t \sim 5000$), spirals diffuse; their maximal size is fixed by the strength of the convective instability and the noise level.

For $c < c_i$, the convective instability is absent and vortex-antivortex pairs are created solely through a “thermal” activation process. (Although this mechanism is also present for $c > c_i$, it does not play a dominant role when the noise is weak.) Since the amplitude of $|a|$ has to be zero at the vortex core, nucleation of a pair requires a rare fluctuation in the noise amplitude, unless it happens next to the core of an existing vortex. Indeed, most of the newly created “thermal” pairs are found next to existing vortices in our simulations. When the noise is weak, the probability for the creation of a thermal pair can be argued to be proportional to an exponential factor, $\exp(-E/T)$, where the “activation energy” E is expected to be lower when next to an existing vortex than in other regions of the system. This is borne out by our simulation data, which show the exponential dependence on T of the ensemble-averaged time τ necessary for the nucleation of a thermal pair from defect-free, tilted initial conditions (Fig. 3a). We also find an almost linear variation of E with phase gradient (Fig. 3b). Moreover, E is found not to be sensitive to the value of c [11].

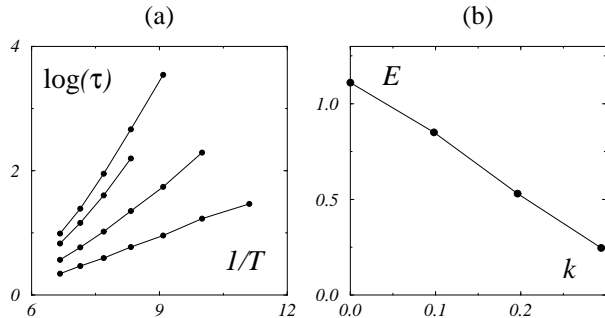


FIG. 3. (a) Logarithm of the average nucleation time τ of a thermal pair of vortices vs. $1/T$ for flat, tilted initial conditions with mean phase gradient k . From top to bottom: increasing k , from $k = 0$ to $k \simeq 0.3$. Each point corresponds to 500 runs of a system of size $L = 128$ at $c = 1.25$. (Even though $c > c_i$, the convective instability has no influence on these results.) (b) Nucleation energy E , as measured from the small T behavior of (a) ($\tau \propto \exp(-E/T)$), vs. k .

In the case of the equilibrium XY model, below the Kosterlitz-Thouless transition temperature [1], vortices of opposite charge attract one another through a logarithmic Coulomb potential and remain bounded in pairs. For $c \neq 0$, however, this attraction is cut off at the distance ξ , beyond which the interaction becomes exponentially weak [8]. Thus, vortices become “free” when their separation is larger than ξ .

For $c \neq 0$ the diffusive motion of individual vortices makes it possible for the nucleated vortices to break away from one another. (Most of them are short-lived, but a fraction do become “free” [11].) On the other hand, it also enables two distant, oppositely-charged vortices to move into the interaction range ξ and annihilate each other. The steady-state density n of free vortices is thus controlled by both the “pumping” rate p of creating vortex pairs of size ξ , and the diffusion constant D which limits the rate of annihilation. On a mean-field level, we can write: $p = Dn^2$. When n is small, we may write $p(n) = p_0 + p_1 n$, where p_0 is the nucleation rate of pairs in the far field, while p_1 is the nucleation rate next to a free vortex. The resulting equation has a unique positive solution, corresponding to a unique steady-state. Our numerical experiments agree with this conclusion: from both synchronized and random initial conditions, a single steady-state seems to be reached [11].

For $c > c_i$, the asymptotic state possesses a nonuniform density of vortices. There are two relevant length scales in this case: the “noise” length $\sim \log(1/T)$ given by noise amplification condition, which determines the size of the large spirals, and the length scale ξ below which vortices of opposite charge annihilate each other. (At such large values of c , ξ becomes comparable to the size of the vortex core.) The system is better described as a gas of large, well-developed spirals with a texture of precipitated vortices at their boundaries [Fig. 2(d)].

In conclusion, we have shown that vortices in the CGLE possess a finite mobility and diffuse under the in-

fluence of an external white noise. The diffusion constant at small noise strength is calculated through a numerical scheme which compares favorably with direct simulations of a noisy CGLE. Our results indicate that the previously observed frozen-defect state of the noiseless CGLE is unstable against noise, and hence it does not possess the kind of metastability exhibited by a typical glassy state. Noise also leads to the creation of free vortices through either an activated process or a dynamic instability. The steady-state of the system becomes unique and contains a finite density of free vortices, in contrast to the behavior of the equilibrium XY model below the Kosterlitz-Thouless temperature.

HC and LHT wish to thank, respectively, the Hong Kong Baptist University and the Materials Science Division, Argonne National Laboratory, for hospitality, where part of this work was performed. The work of IA was supported by the U.S. Department of Energy under contracts W-31-109-ENG-38 (IA) and ERW-E420 and the NSF, Office of STC under contract No. DMR91-20000.

-
- [1] See, e.g.: P. Minnhagen, Rev. Mod. Phys. **59**, 1001 (1987); R.P. Feynman, Prog. Low Temp. Phys. **1**, 17 (1955); M. H. Anderson et al., Science **269**, 198 (1995); D.S. Rokhsar, Phys. Rev. Lett. **79**, 2164 (1997); Yu. Kagan et. al., Phys. Rev. Lett. **76**, 2670 (1996).
 - [2] Y. Kuramoto, *Chemical Oscillations, Waves and Turbulence*, (Springer, Tokyo, 1984).
 - [3] A.T. Winfree, *When Time Breaks Down*, (Princeton University Press, Princeton, 1987).
 - [4] M.C. Cross and P.C. Hohenberg, Rev. Mod. Phys. **65**, 851 (1993), and references therein.
 - [5] For recent experiments, see: Q. Ouyang and J.M. Flesselles, Nature **379**, 143 (1996), and references therein.
 - [6] For a recent account, see: H. Chaté, and P. Manneville, Physica A **224**, 348 (1996); T. Bohr, G. Huber and E. Ott., Europhys. Lett. **33**, 589 (1996)
 - [7] P.S. Hagan, SIAM J. Appl. Math. **42**, 762 (1982).
 - [8] I. S. Aranson, L. Kramer, and A. Weber, Phys. Rev. E **47**, 3231 (1993).
 - [9] I. S. Aranson, L.B. Aranson, L. Kramer, and A. Weber, Phys. Rev. A **46**, R2992 (1992).
 - [10] To determine the eigenfunctions u_α and w_α , we solved simultaneously, using a matching-shooting algorithm, three nonlinear equations for the unperturbed spiral + eight linear equations for the adjoint translation modes.
 - [11] I. S. Aranson, H. Chaté, and L.-H. Tang (in preparation).